

ITERATIVE IMAGE RESTORATION WITH ADAPTIVE REGULARIZATION AND PARAMETRIC CONSTRAINS

SVIATOSLAV VOLOSHYNOVSKIY*

* Faculty of Radio Engineering, State University "Lvivska polytechnika", Lviv, Ukraine

E-mail: svolos@polynet.lviv.ua

Abstract.

In this paper the iterative methods of image restoration are considered. These methods are based on the successive approximation algorithm with adaptive regularization and parametric constrains on the solution. The adaptive regularization preserves the global image smoothing and is considered as the combined nonlinear operator for simultaneous removal of additive Gaussian and impulse noises. The corresponded condition of iteration convergence is investigated. The adaptation strategy is based on the generalized noise visibility function which determines the pixel belonging to the flat arias or edges. Noise visibility function is considered as an indicator function and mathematically determined as the intersection of two additional binary images obtained from local variance estimation and edge image. Extending the previous work, it is proposed the new paparametric constrain on the solution in spatial frequency domain. Opposite the above mentioned regularization, which bounds from above the energy of the restored frequency components, the proposed adaptive frequency constrain determines the lower bound of the solution. The introduction of such constrain is conditioned by the inability of the classical regularized iterative algorithms with the existed constrains to restore the strongly depressed or missed frequency components. To overcome this disadvantage the parametric model of image spectrum is used. The model consists of the sum of 3 exponential decays to approximate the whole image magnitude spectrum using available information about low-pass frequency

part of the degraded image. The proposed approach has the corresponded analogue in the spatial coordinate domain where well-known parametric model of maximum entropy method is used to obtain high spatial resolution. However, opposite maximum entropy model, which is mostly suitable for impulselike images due to its all-poles character, the proposed frequency parametric model has the higher level of generalization, because the exponential model describes the large amount of real image spectra. The performed computer simulation illustrates the high efficiency of the proposed technique on the examples of images degraded by defocusing.

Keywords: adaptive image restoration, regularization, iterative algorithms.

1. Introduction

In many practical imaging systems a recorded image is degraded version of an original image. Degradation is usually conditioned by motion blur, incorrect focusing (defocusing), atmospheric turbulence or diffraction constrains of imaging system. Additionally, blurred image could be noisy that originates from imaging, receiving and recording processes. Image restoration is a procedure of original image recovering from the degraded image using available *apriori* knowledge of blur function and statistics of noise and original image. The restoration problem is one of the most important problems of applied signal processing due to its complexity.

The linear discrete degradation model could be written as 2D convolution of original image f and blur function h

$$g(i, j) = \sum_k \sum_l h(i - k, j - l) f(k, l) + n(i, j) \quad (1)$$

where $g(i, j)$ is the degraded image in coordinates (i, j) . The additive noise n is supposed to be Gaussian, impulse or with mixed distribution. The image is sampled on $M \times M$ equispaced rectangular lattice.

The degradation model (1) could be written as a system of linear equation in operator form for convenience of further analysis

$$g = Hf + n \quad (2)$$

where g , f and n represent the lexicographically ordered noisy blurred image, original image and additive noise, respectively. H represents the linear spatially invariant distortion operator formed from equation (1).

The general solution of image restoration refers to the inverse problem solution which is mostly ill-posed one and has not unique solution. A number of methods are known to provide the solution of the image restoration problem. Their classification could be found in [1, 2, 3]. Despite of different origin of the existed approaches to the solution of restoration problem they are combined by joint ideology of *a priori* information use. *A priori* information could have the diverse nature and mainly includes smoothness of the solution, constrains on the specific image features given in the form of sets and parameters of model which describes the original image and noise. The combination of this information with the received blurred image and degradation model defines a solution. Summarizing consideration of the existed methods we can divide them onto linear and nonlinear.

Linear methods such as Tikhonov regularization [1], Wiener and Kalman filtering [4], methods based on singular value decomposition [2], iterative methods with Tikhonov regularization and controlled quantity of iterations and related methods are not able to solve the problem of band limited extrapolation due to their linear behavior in frequency domain that determines the corresponded possible enhancement of spatial resolution. These methods use mostly information about smoothness of the solution expressed in the form of stabilization functional (Tikhonov regularization), ratio of image to noise power spectra (Wiener filtering) or corresponded quantity of iterations which restricts the level of high frequency components in the restored image.

Nonlinear methods are potentially able to create the new frequency components in the spectrum of the restored image different from the components in the spectrum of blurred image and can solve the bandlimited extrapolation problem. The nonlinear methods could be divided on two large groups according to the practical realization of the minimization scheme of a compound functional which combines the information about degradation model, smoothness of the solution, *a priori* constrains on the nonnegativity and spatial image extent, covariance matrices or power spectra of original image and noise, corresponded image and noise variance, image spatial symmetry, and information about original image expressed in the form of some parametric model (autoregressive or maximum entropy models, Markov chains). The first group includes the methods of direct compound functional minimization originating from optimization ideology and the second one combines the methods based on the iterative algorithms of linear equation system solution with regularization and constrains on the solution which are known as methods with projection onto convex sets (POCS). Obviously,

both linear and nonlinear methods could be derived from the general scheme of compound functional minimization in dependence on the kind of used information.

In this paper the iterative methods with regularization and constrains on the solution are considered due to their advantages over other existed restoration techniques. Briefly summarizing main advantages of the regularized iterative methods with constrains on the solution we can indicate their ability simultaneously to combine mathematical simplicity of programming, nonlinearity (i.e. ability to extrapolation), the possibility to take into account the image local structure (i.e. spatial or frequency adaptivity), robustness against the errors in blurring operator, existence of the strict convergence condition and mathematical expressions for the error of the image restoration. The most computational complicated operations consist in the calculation of 2D convolutions that could be easily performed by means of specialized digital or optical processors and algorithms based on the fast Fourier transform (FFT).

However, these methods have some disadvantages linked with the low convergence rate of iterations in the case of strong degradation, ringing effect near edges, global character of image smoothing and high sensitivity to impulse noise. To overcome these disadvantages the adaptive-parametric approach is proposed in this paper. The paper has the following structure. The general theory and evolution of regularized iterative algorithms is considered in Section 2. The adaptive-parametric approach is presented in Section 3. Experimental results and comparative analysis are performed in Section 4, and Section 5 concludes the paper.

2. Iterative image restoration algorithms

2.1. The evolution of iterative restoration algorithms

The base scheme of iterative image restoration is the method of successive approximation which is often applied to the solution of linear algebraic system of equations [5]

$$\hat{f}^{k+1} = \hat{f}^k + \beta H^T (g - H\hat{f}^k) \quad (3)$$

$$\hat{f}^0 = \beta H^T g$$

where \hat{f}^{k+1} is the estimation of f on $k+1$ iteration, β is a relaxation parameter, “ T ” denotes matrix transpose and $\|\cdot\|$ is matrix norm. The relaxation parameter controls the convergence of iterations and is determined as

$$0 < \beta \leq 2\|H^T H\|^{-1}. \quad (4)$$

The solution obtained after infinite number of iterations converges to the result of inverse filtering. To constrain the influence of noise the finite number of iterations was usually chosen that was the first way of regularization in iterative methods.

The introduction of the general regularization theory into iterative process allowed to essentially increase the algorithm noise immunity. The generalized scheme of iterative method with Tikhonov regularization could be written as [4]

$$\begin{aligned} \hat{f}^{k+1} &= (I - \alpha\beta C^T C)\hat{f}^k + \beta H^T (g - H\hat{f}^k) = \\ &= (I - \beta(H^T H + \alpha C^T C))\hat{f}^k + \beta H^T Hg \end{aligned} \quad (5)$$

where α is a regularization parameter, C represents high-pass filter obtained from Tikhonov stabilization functional, I is unit matrix. The corresponded condition for relaxation parameter is

$$0 < \beta \leq 2\|H^T H + \alpha C^T C\|^{-1}. \quad (6)$$

A.Katsaggelos *at al.* [6] established that operator $(I - \alpha\beta C^T C)$ represents the low-pass filter that smoothes restored image to prevent noise fluctuations in the solution and it is soft constrain on smoothness

$$\begin{aligned}\hat{f}^{k+1} &= C_S \hat{f}^k + \beta H^T (g - H \hat{f}^k) = \\ &= (C_S - \beta H^T H) \hat{f}^k + \beta H^T H g\end{aligned}\quad (7)$$

where $C_S = I - \alpha\beta C^T C$. It was proposed to change it on Wiener filter for optimal filtering.

To avoid the global image smooth and to make restoration adaptive to the local image structure the generalized iterative method was proposed [3, 7, 8, 9]

$$\hat{f}^{k+1} = C_S \hat{f}^k + \beta H^T W (g - H \hat{f}^k) \quad (8)$$

where $C_S = I - \alpha\beta C^T S C$, and W and S are known diagonal weight matrices with positive elements. It was proposed to determine W and S using *noise visibility function (NVF)* which is inverse to local variance [8, 10] as

$$\begin{aligned}s(i, j) &= NVF(i, j), \\ w(i, j) &= 1 - NVF(i, j).\end{aligned}\quad (9)$$

The properties of the *NVF* are described in more details in subsection 2.2. We have selected this scheme as a separate class of algorithms, because it determines the generalized direction in the range of this paper.

The considered above algorithms were linear ones. Despite of new adaptation ideology none regularization is potentially able to increase the resolution, because ensuring the stability of the solution it automatically smoothes image. In the boundary case, when noise decreases to zero the regularization influence should also be the minimal one. Although, even in the case of the high signal-to-noise ratio (SNR) the above iterative algorithms are not able to restore image uniquely due to their inability

to restore missed or strongly depressed frequency components of degraded image.

The introduction of the constrains makes possible to create the nonlinear algorithms able to solve the bandlimited extrapolation problem. Unfortunately, not so many constrains exist that could be used in the general cases of strongly degraded image restoration. The art of constrains application were mainly developed in the range of POCS ideology. The generalized scheme of iterative method with regularization and constrains on the solution could be written

$$\begin{aligned}\hat{f}^0 &= \beta H^T g, \\ \hat{f}^{k+1} &= C_S \mathfrak{R}[\hat{f}^k] + \beta H^T W (g - H \mathfrak{R}[\hat{f}^k])\end{aligned}\quad (10)$$

where \mathfrak{R} is the set of projection operators $\mathfrak{R} = C_N C_{ext} C_M C_\phi$ onto the corresponded sets of constrains: C_N is constrain on the intensity range of possible solutions with the fixed lower and upper bounds, C_{ext} is the constrain on the spatial image extent, C_M and C_ϕ are constrains on *a priori* given module and phase of the solution, respectively. The features of these constrains and the proof of convexity are well-studied [11]. Therefore, we only summarize their main particularities needed for the development of parametric constrain ideology.

i. The constrain on the intensity range is efficient mostly for impulselike signals and images in spectroscopy and astronomy. In the general case of complex image structure which combines the flat arias and impulse objects, that is common for real photo, radiometry or medical images with different nature, the efficiency of this constrain is not very high and the restored image is not much better in comparison with the image obtained without this constrain.

ii. The constrain on the spatial image extent is also efficient for astronomy where it is possible to localize the object in some area. It was proven that this constrain alone could provide the unique image restoration in the case of noise absence [11]. The application of such constrain could be also useful for text document restoration to reduce the ringing effect, if text area could be localized [12]. However, in the general case of complex images it is not possible to set such extent bounds.

Therefore, it was proposed in our previous work to use the modified constrain which took into account the local image structure and combines features of two constrains considered above [13], i.e. ability to constrain the local intensity range that could be considered as the constrain on the spatial extent generalized on the case of complex images.

iii. The large amount of publications are devoted to the image restoration from its module, i.e. so-called phase problem [3, 11]. It is stated that this problem could be solved uniquely especially for 2D image. The experiments performed in this work have shown that the constrain on module does restore image, if some information about phase is available in the degraded image. If phase information is completely absent this constrain did not confirm the expected results. Moreover, the module constrain is very seldom known *a priori* excluding some specific cases. Therefore, in this paper the parametric approach is proposed to estimate the module constrain and avoid the lack of *a priori* information.

iv. The constrain on phase is the most powerful one among the above considered constrains. The numerous practical experiments show that incorporating the *a priori* phase information with the averaged module of the group of images it is possible to obtain the satisfactory image restoration in the most cases. Unfortunately, we can not indicate many systems

where *a priori* phase information is completely available. Although, a typical situation is observed for imaging systems which save phase information in nonzero areas of spatial spectrum and lose it when transfer function is equal to zero. The examples of such degradation are motion blur and defocusing. Therefore, the essential part of phase information is saved and the problem is to develop the adequate constrain on module. The approach proposed in this paper is especially useful in these situations.

2.2. Choice of *NVF*

Taking into account the masking effect of *human visual system (HVS)* Anderson and Netravali [14] proposed to use *NVF* to adopt restoration algorithm to the local image structure. The main idea was to express the mathematical relationship between the visibility of noise on the flat regions and its masking near edges. This approach has found its further development in the algorithms like (8), where *NVF* was proposed to be calculated using the local variance as a measure of the spatial details. Although, such kind of adaptation allowed to obtain results better than the nonadaptive regularization, authors indicated on the necessity of further investigation of optimum parameters of this method, and namely optimum number of thresholds and their values, normalization tuning parameter and parameter of regularization [8]. Moreover, *NVF*, calculated on the base of local variance inversion, performs the smoothed estimation of edges that leads to the corresponded rough estimation of fine details. Additionally, such *NVF* was estimated either directly from noisy degraded image or from partially restored image. Taking into account smoothed edges and noise in the mentioned images the smoothing property of local variance caused the appearance of false details that were considered as the right detected edges in *NVF*. The tendency was increased with the decrease of SNR that leads to the completely unrecognizable original image and the

corresponded inefficiency of the proposed *NVF*. Moreover, in the case of impulse noise even with density 10-20% of general pixel quantity the resulted *NVF* will be about uniform. Obviously, in this case such *NVF* can not supply the adaptation scheme by the necessary information.

Taking into account the above disadvantages we propose to consider *NVF* as the result of image segmentation into two regions R_1 (edge region) and R_2 (flat arias). *NVF* is equal to 0 for areas with high spatial activity (i.e. edges), where noise is not visible for human vision system, and equal to 1 for flat arias where noise is visible. *NVF* is propose to be calculated as the intersection of two images obtained from modified local variance and edge image. The modified local variance is not so sensitive to impulse noise as the operator of edge extraction, but it is too smooth in the edge regions while image obtained from edge extraction is more precise there. *NVF* is used further as an indicator function to adopt the parameters of the restoration algorithm to the local image structure. According to segmentation ideology *NVF* could be written

$$NVF(i, j) = \begin{cases} 0, & \text{if } f(i, j) \in R_1, \\ 1, & \text{if } f(i, j) \in R_2. \end{cases} \quad (11)$$

We propose to determine R_1 and R_2 using the next conditions

$$\begin{aligned} R_1 &\equiv \{(i, j) | \sigma_{\hat{f}}(i, j) > T_{\sigma} \cup \text{edge}(\hat{f}(i, j)) > T_e\}, \\ R_2 &\equiv \{(i, j) | \text{otherwise}\}, \end{aligned} \quad (12)$$

where $\sigma_{\hat{f}}(i, j)$ is the modified local variance and $\text{edge}(\hat{f}(i, j))$ is the operator of edge extraction for coordinates (i, j) , T_{σ} and T_e are thresholds for local variance and edge image binarization.

The modified local variance is defined by

$$\sigma_{\hat{f}}(i, j) = \frac{1}{N} \sum_{(k, l) \in \Omega} (\hat{f}(i+k, j+l) - \bar{f}(i, j))^2 \quad (13)$$

where

$$\bar{f}(i, j) = \frac{1}{N} \sum_{(k, l) \in \Omega} \hat{f}(i+k, j+l) \quad (14)$$

is local mean, Ω is rectangular window of pixels centered at (i, j) and with N the total number of pixels, $\hat{f}(i, j)$ is previously restored image or image from previous iteration. To reduce the influence of impulse noise we propose to perform the prefiltering of $\hat{f}(i, j)$ to use modified image $\tilde{f}(i, j)$ instead of $\hat{f}(i, j)$ in (13) and (14)

$$\tilde{f}(i, j) = \begin{cases} \text{med}(\hat{f}(i, j)), & \text{if } \hat{f}(i, j) = f_{\min} \\ & \text{or } \hat{f}(i, j) = f_{\max}, \\ \hat{f}(i, j), & \text{otherwise} \end{cases} \quad (15)$$

where $\text{med}(\hat{f}(i, j))$ denotes the median filter. It is assumed that the salt and pepper model of impulse noise is used that predicts noised pixels could have only f_{\min} or f_{\max} values of the image. This *priori* information accompanied by knowledge of flat arias and edges could be efficiently used for impulse noise reduction not only in *NVF* but also in smoothing operator which performs the function of regularization that is considered below.

To design the operator of edge extraction $\text{edge}(\hat{f}(i, j))$ anyone well-known method could be used [1]. Moreover, to estimate edges more precisely and avoid the noise influence, which will appear on the binarized image as the separated points, the morphological analysis could be performed here to determine the edge connectivity. In our approach the

two-component model [15] was used to determine operator $edge(\hat{f}(i, j))$ due to its simplicity of calculation and wide use in applied signal processing algorithms. Moreover, this approach will be used for parametric constrain below too. The *two-component model* predicts that the initial image could be considered to consist of two parts: a low frequency $\bar{f}(i, j)$ and high-frequency part that is equal to the difference of $(\hat{f}(i, j) - \bar{f}(i, j))$ that represents the edges in the initial image. Determine the edge operator as

$$edge(\hat{f}(i, j)) = |\hat{f}(i, j) - \bar{f}(i, j)| \quad (16)$$

where $|\cdot|$ denotes the absolute value.

The thresholds T_σ and T_e in (12) defines the level of desired image details and are determined experimentally. The typical values used in our image segmentation are $T_\sigma = (0.08 \div 0.1)f_{\max}$, $T_f = (0.04 \div 0.08)f_{\max}$.

2.3. Generalized structure of C_S

We propose to consider the regularization as a generalized smoothing of the image that could be accomplished by any known method of noise removal, i.e. by neighborhood filter, classical regularization smoothing or Wiener filter, adaptive filters, median etc.

In the case of usual neighborhood averaging filter smoothing operator will be

$$C_S \hat{f}^k = \frac{1}{N} \sum_{(k,l) \in \Omega} \hat{f}^k(i+k, j+l). \quad (17)$$

Smoothing filter based on regularization approach or Wiener filtering could be written as

$$C_S = I - \alpha \beta C^T C \quad (18)$$

$$C_S = S_{ff} (S_{ff} + S_{mn})^{-1} \quad (19)$$

where S_{ff} and S_{mn} are covariance matrices of the initial image and noise which supposed to be known *a priori*. If these matrices were known *a priori*, it would be possible to use this information not only for image smoothing, but also for phase retrieval that could lead to better results. Unfortunately, this situation happens very seldom in practice.

Although, the above methods have been used for a long time due to simplicity of smoothing problem formulation and corresponded solution they have the common disadvantage linked with the edge degradation caused by global smooth ideology. Edge preserving ideology of adaptive filtering conditioned the appearance of new generation of smoothing filters. The above considered example (8) based on weight matrix S shows the main structure of such filters

$$C_S = I - \alpha \beta C^T S C. \quad (20)$$

The considered filters are designed for Gaussian noise removal and are inefficient in the case of impulse or mixed noise. A version of iterative methods regularization based on median or trimmed mean filtering was proposed in our previous work [16]

$$C_S \hat{f}^k = med(\hat{f}^k). \quad (21)$$

The new frontiers in impulse noise removal are linked with pixel identification techniques which determine noise suspected points [17] and provide only their filtering to prevent image global smoothing. This idea was partially used in the above considered modified local variance. Therefore, expected future success that could be reached in the direction of the development of new methods for adaptive regularization is strictly linked with new achievements in noise removal algorithms.

3. Adaptive-parametric approach

3.1. The choice of adaptive operator C_S for simultaneous Gaussian and impulse noise removal

We propose to use here the combined version of adaptive filter based on edge preserving neighborhood averaging filter for Gaussian noise removal and adaptive median filter based on the pixel identification technique with adaptive window in dependence on the local image structure for impulse noise removal (salt and pepper model). The local image structure for adaptation is determined by the considered above NVF .

According to it the new combined smoothing operator C_S is defined by

$$C_S \hat{f}^k(i, j) = \begin{cases} \text{med}(\hat{f}^k(i, j)), & \text{if } \hat{f}^k(i, j) = f_{\min} \\ & \text{or } \hat{f}^k(i, j) = f_{\min}, \\ \hat{f}^k(i, j), & \text{if } NVF(i, j) = 0, \\ \bar{f}^k(i, j), & \text{if } NVF(i, j) = 1 \end{cases} \quad (22)$$

where

$$\bar{f}^k(i, j) = \frac{1}{N} \sum_{(k,l) \in \Omega} \hat{f}^k(i+k, j+l) \quad (23)$$

is updated on every iteration and Ω is rectangular window with size 3×3 . Another approach consists in the modification of the impulse noise reduction part of previous one. To reduce the influence of impulse noise on Gaussian noise filtering on flat arias it is proposed to use the averaging of only impulse noise free pixels

$$\bar{f}^k(i, j) = \frac{1}{N'} \sum_{(k,l) \in \Omega} \hat{f}^k(i+k, j+l),$$

if $\hat{f}^k(i+k, j+l) \neq f_{\min}$ (24)
or $\hat{f}^k(i+k, j+l) \neq f_{\max}$

where N' is the total number of impulse noise free pixels. If all pixels in window 3×3 are impulse noise

corrupted, i.e. have minimal and maximal values opposite flat aria with only minimal or maximal values, and N' is equal to zero, window size is increased to 5×5 . If the above situation is repeated the window size is increased to 7×7 that could be only for strongly impulse noisy images (i.e. noise density is above 30% of general quantity of image pixels). Obviously, the same ideology could be used for filtering of only Gaussian noise corrupted pixels that will essentially decrease the undesirable image smoothing and reduce the general quantity of needed operations. However, this problem requires additional investigation to determine the corresponded optimal level of thresholds in dependence on *apriori* given noise variance to detect noise corrupted pixels.

3.2. Condition of iteration convergence

Consider the convergence condition of the proposed algorithm with adaptive nonlinear filter C_S and weight matrix W . The distance between the functions in L_2 space is

$$\| (C_S - \beta H^T W H)(f_1 - f_2) \| = \left\{ \int_{-\infty}^{\infty} |C_S(\omega) - \beta W(\omega) H(\omega)|^2 |F_1(\omega) - F_2(\omega)|^2 d\omega \right\}^{\frac{1}{2}}$$

where $C_S(\omega)$, $W(\omega)$, $H(\omega)$, $F_1(\omega)$ and $F_2(\omega)$ are corresponded frequency domain analogues of C_S , W , H , f_1 and f_2 . It is assumed that ω denotes the corresponded spatial frequencies $\omega = (\omega_i, \omega_j)$ for both spatial coordinates.

The sufficient conditions for iteration convergence is

$$|C_S - \beta H^T W H| < 1.$$

That is equal to

$$|C_S(\omega) - \beta W(\omega) H(\omega)|^2 < 1.$$

The above inequality makes possible to determine the corresponded relaxation parameter bounds:

$$\frac{C_s(\omega) - 1}{W(\omega)|H(\omega)|^2} < \beta < \frac{C_s(\omega) + 1}{W(\omega)|H(\omega)|^2} \quad (25)$$

Taking into account the low-pass character of C_s we can write

$$0 \leq C_s(\omega) \leq 1. \quad (26)$$

Then we obtain the next estimation for lower and upper bounds

$$\begin{aligned} C_s(\omega) = 0: \\ -\left(W(\omega)|H(\omega)|^2\right)^{-1} < \beta < \left(W(\omega)|H(\omega)|^2\right)^{-1}, \\ C_s(\omega) = 1: 0 < \beta < 2\left(W(\omega)|H(\omega)|^2\right)^{-1}. \end{aligned}$$

The intersection of these sets gives the condition for the choice of relaxation parameter

$$0 < \beta < \frac{1}{\max\left[W(\omega)|H(\omega)|^2\right]}. \quad (27)$$

3.3. Parametric constrains on the solution

As it was mentioned in subsection 2.1 only two constrains could be directly available on practice, i.e. constrain on the range of the possible gray levels with the fixed bounds and some information about module of the spectrum until cut-off frequency that is not enough for the satisfactory image restoration. Therefore, the necessity appears to use constrains based on the parametric model of the image to compensate the lack of *a priori* information.

The generalized algorithm with the constrains on adaptive range of the possible gray levels and module of image spectrum could be written as

$$\hat{f}^{k+1} = C_s \mathfrak{R}[\hat{f}^k] + \beta H^T W (g - H \mathfrak{R}[\hat{f}^k]) \quad (28)$$

where $\mathfrak{R} = C_N C_M$. Operator C_s is defined by (22).

As the first iteration we propose to choose

$$\hat{f}^0 = \beta H^T \mathfrak{R}[g] \quad (29)$$

which alone could give better results in comparison with the usual method even without further constrains.

The main features of the proposed algorithm are determined by the structure of the constrains. In [13] it was proposed to use the parametric constrain to restrict the possible range of solutions

$$C_N[\hat{f}^k] = \begin{cases} \hat{f}^k, & \text{if } B_L \leq \hat{f}^k \leq B_U, \\ B_L, & \text{if } \hat{f}^k < B_L, \\ B_U, & \text{if } \hat{f}^k > B_U. \end{cases} \quad (30)$$

where

$$\begin{aligned} B_L &= \hat{f}^k - T_B, & \text{if } \text{edge}(\hat{f}^k) < T_e, \\ B_U &= \hat{f}^k + T_B, & \text{if } \text{edge}(\hat{f}^k) > T_e \end{aligned}$$

and $T_B \leq T_e$, T_B is the threshold which determines the level of desired details in the restored image edges and possible level of noise fluctuations. However, in the case of strongly degraded image this constrain could not exactly determine the lower bound of solution in frequency domain. Therefore, it is proposed to define the lower bound directly in frequency domain using next constrain on module

$$C_M[\hat{f}^k] = \begin{cases} \mathfrak{S}^{-1}\{|\hat{F}_L(\omega)|\}, & \text{if } |H(\omega)|^2 \leq T_z, \\ \mathfrak{S}^{-1}\{|\hat{F}^k(\omega)|\}, & \text{if } |H(\omega)|^2 > T_z, \end{cases} \quad (31)$$

$$|\hat{F}_L(\omega)| = \left(|\hat{F}_{apr}(\omega)| + |\hat{F}^k(\omega)| \right) / 2,$$

$$T_z = 0.1 \max |H(\omega)|^2 = 0.1 |H(0)|^2$$

where $|\hat{F}_{apr}(\omega)|$ is the estimation of the mean amplitude spectrum of the initial image and $\mathfrak{S}^{-1}\{\cdot\}$ denotes inverse Fourier transform.

To estimate this mean spectrum the parametric model was used. This model is based on the fact that most of

spectra of real images have the exponential decay character. The model of the sum of 3 exponential decays was used. The same methodology could be noted to exist in applied spectral analysis where maximum entropy model is used to approximate the spectrum of the signal. According to the proposed method the estimation of the mean spectrum of image amplitude spectrum is modeled by

$$\left| \hat{F}_{apr}(\omega) \right| = \sum_{p=1}^3 a_p e^{-\frac{\omega}{\gamma_p}} \quad (32)$$

where $\{a_p\}$ and $\{\gamma_p\}$ are parameters of the model which are found on the base of the functional minimization:

$$\Phi[a, \gamma] = \left\| \hat{F}'(\omega) - \hat{F}_{apr}(\omega) \right\| + \lambda C[a, \gamma] \quad (33)$$

where λ is Lagrangian multiplier, $C[a, \gamma]$ is constrain on the possible ranges of the values of $\{a_p\}$

and $\{\gamma_p\}$ obtained from the averaged spectrum of the group of images, $\hat{F}'(\omega)$ is the estimation of the initial image spectrum in the range of cut-off frequency $\omega_{cut-off}$ of the imaging system taken on the level of

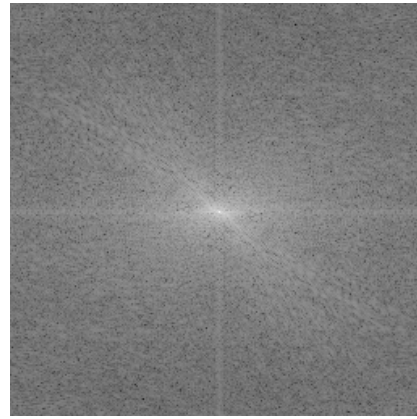
$$\hat{F}'(\omega) = G(\omega) / \left(|H(\omega)|^2 + \alpha |C(\omega)|^2 \right), \quad (34)$$

if $|\omega| \leq \omega_{cut-off}$.

Therefore, on the base of available low-pass part of the degraded image, which alone does not guarantee the satisfactory restoration, the lower bound of module extended on whole frequency domain is found.



a



b

Fig. 1. Test image “Lena” (a) and its spatial spectrum (b).

4. Computer modeling

A number of experiments have been performed to investigate the main features of the proposed algorithm. Some of these results are presented in this section. The “test” image “Lena” with size 256x256 pixels (Fig. 1a) was chosen for comparison reasons due to its wide use in the corresponded papers. The spatial spectrum of this image is shown in Fig. 1b. The spatial spectrum is normalized to 256 gray level scale and displayed as the function

$$D(\omega) = \log_{10}(1 + F(\omega)) \quad (35).$$

The modeling is divided on two parts. The first part is to show the possibilities of the proposed restoration algorithm in comparison with the mostly used technique based on iterative scheme with Tikhonov regularization and constrain on nonnegativity on the

example of strongly degraded image with high signal-to-noise ratio (SNR). The second part investigates the immunity of the restoration algorithms against mixed (i.e. Gaussian and impulse) noise.

4.1. Restoration of strongly degraded image with high SNR

This part includes consideration of practically important case of image restoration with defocusing degradation. The most of papers refer to defocusing with radius of pill-box model R equals less then 9 pixels [4, 10]. Therefore, we consider defocusing with $R=9$ and strong degradation with defocusing $R=50$. The level of image degradation is estimated as the normalized square error between original image f and degraded image g that is defined by

$$\delta_g = \frac{\|f - g\|}{\|f\|}. \quad (36)$$

The resulting blurred-signal-to-noise ratio (BSNR) on the degraded image was estimated as

$$\Delta_{BSNR} = 10 \log_{10} \frac{\|g'\|}{\|g - g'\|} \quad (37)$$

where g' is noise free degraded image.

The performance of restoration algorithm is estimated by measuring the restoration error defined by normalized square error between original image f and restored image \hat{f}^k

$$\delta_{\hat{f}} = \frac{\|f - \hat{f}^k\|}{\|f\|}. \quad (38)$$

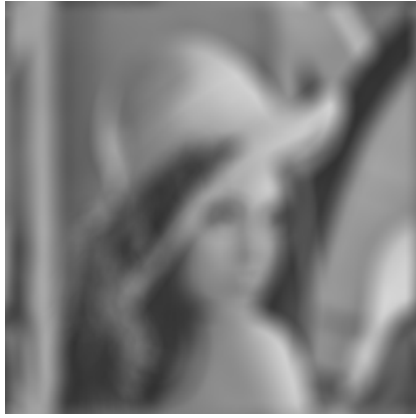
The first experiment consists in the restoration of ‘‘Lena’’ blurred by defocusing with $R=9$. The defocused image is shown in Fig. 2a and the corresponded spectrum in Fig. 3a. The degradation error was 18.32%. The quantization effect conditioned quantization errors and BSNR was equal to 53 dB.

The result of image restoration by means of iterative method (10) with adaptive Tikhonov regularization and constrain on nonnegativity after 50 iterations is shown in Fig. 2b and the corresponded spatial spectrum of this image is shown in Fig. 3b. The relaxation parameter was chosen $\beta=2$ for comparison reason for all restorations. The tuning parameter θ for calculation of NVF was chosen 0.01 in accordance with [8]. The window was nonadaptive and matrices W and S were constant. The operator C was chosen as the Laplasian operator and calculated as the mask:

0	-1	0
-1	4	-1
0	-1	0

The error of restoration was 12.41%. The level of high frequency components in spatial spectrum of the restored image does not correspond to the level of frequency components in the original image that is conditioned by the mentioned inability of such algorithms to restore highly depressed frequency components. As a result we observe ‘‘ringing’’ effect on the restored image that caused the decrease of spatial resolution.

To eliminate this disadvantage the proposed algorithm with lower spectrum bound estimation based on constrain (31) and spectrum model (32) was used. The result of image restoration after 25 iterations is shown in Fig. 2c and corresponded spectrum in Fig. 3c. The error of image restoration was 7.85%. Comparing the spatial spectra from Figs. 3b and 3c we can note that the last spectrum has essentially higher level of high frequency components than the previous one that is determine by the introduced lower bound.



a

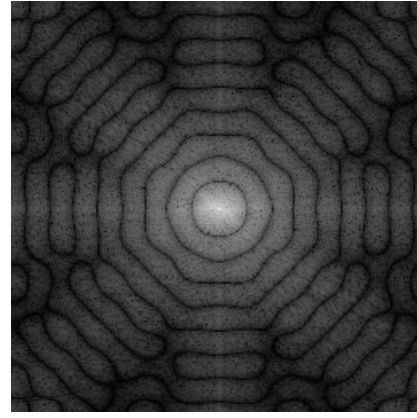


b

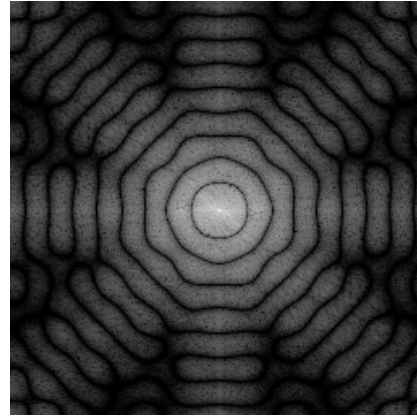


c

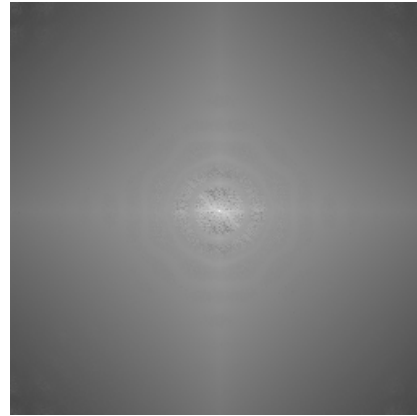
Fig. 2. Original image “Lena” degraded by defocusing with radius of pill-box model equals 9 (a) ($\delta_g = 18.32\%$) and quantization noise with BSNR 53 dB; image restored by means of the iterative method with adaptive regularization and constrain on nonnegativity (b) ($\delta_f = 12.41\%$); image restored by means the proposed algorithm (c) ($\delta_f = 7.85\%$).



a



b



c

Fig. 3. Spatial spectra of images shown in Fig. 2.

The next experiment demonstrates the results of image restoration for defocusing with $R=50$. The blurred image is shown in Fig. 4a and its corresponded spectrum in Fig. 5b. Visually it is difficult to recognize the original image in the blurred one. The error of image degradation was $\delta_g = 32.57\%$ and BSNR=53 dB. The same set of restorations as for Fig. 3 was performed for this level of image distortion too. The error of image restoration for Fig. 4b was $\delta_f = 27.47\%$ after 50 iterations and for image from Fig. 4c $\delta_f = 15.77\%$ after 25 iterations by means of the corresponded algorithms described in the above. The spectra of the blurred and restored images are shown in Fig. 6. Thus, both visually and qualitatively according to the chosen criterion the proposed algorithm gives better results in comparison with algorithm without constrain on lower bound of image spectrum.

4.2. Restoration of image degraded by mixed noise

In this set of restorations the main aim was to investigate the immunity of the proposed algorithm against the Gaussian and impulse noise. The original image “Lena” was blurred by defocusing with $R=9$. White Gaussian noise was added so that BSNR was equal to 30 dB. Then this image was corrupted by impulse noise (salt and pepper model) with probability of spike appearance equals 5% for image from Fig. 7a and 50% for image from Fig. 8a. The resulting BSNR estimated according to (37) were 12.76dB and 2.77dB for image from Figs. 7a and 8a, respectively. The last two images were used for further restoration.

Taking into account inability of the considered above algorithm (10) to restore image with radius of pill-box 9 with high BSNR the further modeling is only performed for the proposed algorithm. Moreover, adaptive Tikhonov regularization is not suitable for

impulse noise filtering. The main part of restoration scheme is noise reduction scheme. In all further restorations the adaptive smoothing operator (22) with modified averaging part (24) was used. *NVF*, used in (22), was computed according to segmentation schemes (11) and (12). The performance of the proposed technique is presented in Figs. 7 and 8. The results of image restoration with the proposed smoothing operator and constrain on lower bound estimated according to (31) after 25 iterations are shown in Figs. 7b and 8b for 5% and 50% impulse noises, respectively. The error of image restoration for the above images were 9.86% and 11.96%. Therefore, comparing the last images with the corresponded result obtained for high BSNR (Fig. 2c) one can see that error of image restoration increased not so much as decreased BSNR that show the high level of noise immunity of the proposed algorithm for simultaneous influence of Gaussian and impulse noises.

To evaluate the potential abilities of the proposed technique the restoration with completely known amplitude spectrum of original image and the proposed smoothing operator was performed. The corresponded results of image restoration after 25 iterations are shown in Figs. 7c and 8c for 5% and 50% impulse noises, respectively. The errors of image restoration were 7.16% and 10.42%. Comparing the restoration with the known *priori* amplitude spectrum and spectrum estimated according to the proposed parametric model we can conclude that the error of image restoration is a little bit lower in the first case. If the information about amplitude spectrum were available in practice, it could efficiently incorporated in the proposed algorithm. However, due to the lack of this information we can suppose that the proposed model of amplitude spectrum can give satisfactory results even for strongly defocused and noisy images.



a

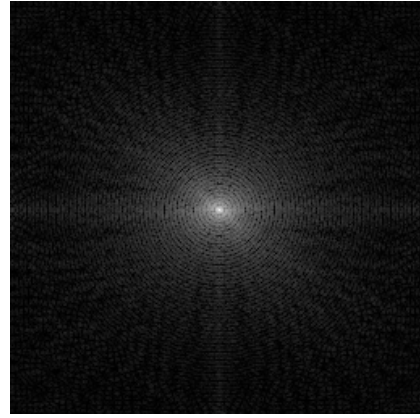


b

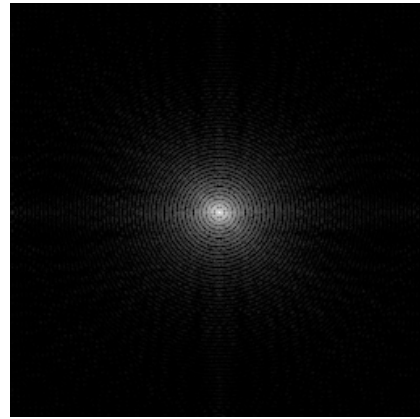


c

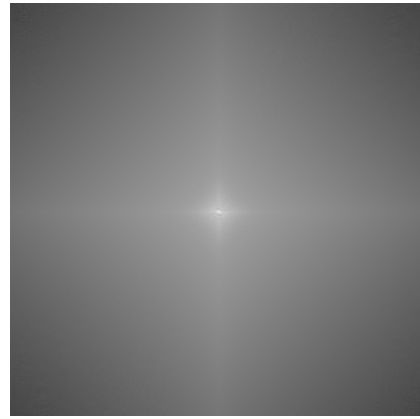
Fig. 5. Original image “Lena” degraded by defocusing with radius of pill-box model equals 50 (a) ($\delta_g = 32.57\%$) and quantization noise with BSNR 53 dB; image restored by means of the iterative method with adaptive regularization and constrain on nonnegativity (b) ($\delta_f = 27.47\%$); image restored by means of the proposed algorithm (c) ($\delta_f = 15.77\%$).



a

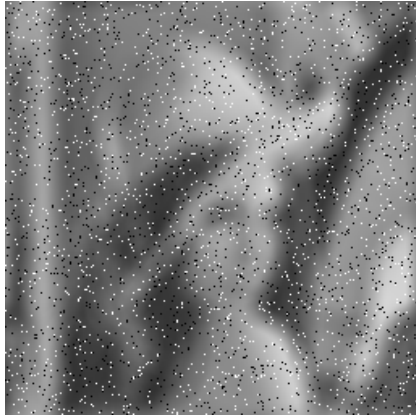


b



c

Fig. 6. Spatial spectra of images shown in Fig. 5.



a

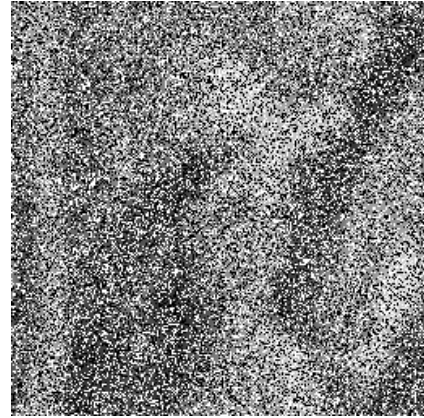


b



c

Fig. 7. Original image “Lena” degraded by defocusing with radius of pill-box model equals 9 and corrupted by Gaussian noise with BSNR=30 dB and 5% impulse noise (a); image restored by means of the proposed algorithm (b) ($\delta_f = 9.86\%$); image restored using the proposed smoothing operator and *a priori* amplitude spectrum (c) ($\delta_f = 7.16\%$).



a



b



c

Fig. 8. Original image “Lena” degraded by defocusing with radius of pill-box model equals 9 and corrupted by Gaussian noise with BSNR=30 dB and 50% impulse noise (a); image restored by means of the proposed algorithm (b) ($\delta_f = 11.96\%$); image restored using the proposed smoothing operator and *a priori* amplitude spectrum (c) ($\delta_f = 10.42\%$).

5. Conclusions

In this paper the adaptive-parametric approach to image restoration is proposed. The generalized adaptive regularization is introduced as the smoothing adaptive filter for simultaneous removal of Gaussian and impulse noises. The adaptive filter is updated on every iteration according to the estimation of local signal activity given as NVF . The condition of iteration convergence is considered. The modified NVF is proposed as the intersection of two additional binary images obtained from local variance and edge extraction. The new parametric constrain on module of the restored image spectrum is proposed.

References

- [1] Gonzalez R.C, Wintz P., *Digital Image Processing*, Addison-Wesley, Massachusetts, 1992.
- [2] Andrews H.C., Hunt B.R., *Digital Image Restoration*, Prentice Hall, New York, 1977.
- [3] Sezan M.I., Tekalp A.M., "Survey of Recent Developments in Digital Image Restoration", *Optical Engineering*, vol. 29, No. 5, pp. 393-404, 1990.
- [4] Biemond J., Lagedijk R.L., Mersereau R. M., "Iterative Methods for Image Deblurring", *IEEE Trans.*, vol. 78, No. 5, pp. 856-883, 1990.
- [5] Ortega J. M., *Introduction to Parallel and Vector Solution of Linear Systems*. Plenum Press, New York, 1988.
- [6] Katsaggelos A.K., Biemond J., Mersereau R.M., and Schafer R.W., "A General Formulation of Constrained Iterative Restoration Algorithms", *Proc. IEEE Int. Conf. Acoustics, Speech, Signal Processing*, pp. 700-703, 1985.
- [7] Kang M.G., Katsaggelos A.K., "Simultaneous Iterative Image Restoration and Evaluation of the Regularization Parameter", *IEEE Trans. on Signal Processing*, vol. 40, No. 9, pp. 2329-2334, 1992.
- [8] Efstratiadis S. N., Katsaggelos A.K., "Adaptive Iterative Image Restoration with Reduced Computational Load", *Optical Engineering*, vol. 29, No. 12, pp. 1458-1468, 1990.
- [9] Sezan M.I. and Tekalp A.M., "Adaptive Image Restoration with Artifact Suppression using the Theory of Convex Projections", *IEEE Trans. Acoustics, Speech, Signal Processing*, vol. 38, pp. 181-185, Jan. 1990.
- [10] Katsaggelos A.K., Biemond J., Schafer R.W., and Mersereau R.M., "A Regularized Iterative Image Restoration Algorithm", *IEEE Trans. on Signal Processing*, pp. 914-929, 1991.
- [11] Schafer R.W., Mersereau R.M., Richards M.A., "Constrained Iterative Restoration Algorithms", *Proc. IEEE*, vol. 69, No. 4, pp. 432-450, 1981.
- [12] Lagedijk R.L., Biemond J., and Boeke D.E., "Regularized Iterative Image Restoration with Ringing Reduction", *IEEE Trans. Acoustics, Speech, Signal Processing*, vol. 36, pp. 1874-1888, Dec. 1988.
- [13] Prudius I., Grytskiv Z., and Voloshynovskiy S., "Radiometry Image Processing based on Nonlinear Iterative Methods," *Proc. Workshop on Design Methodologies for Signal Processing*, Zakopane, Poland, pp.21-27, Aug. 1996.
- [14] Anderson G.L. and Netravali A.N., "Image Restoration based on a Subjective Criterion", *IEEE Trans. Syst., Man, Cyber, SMC-6*, pp. 845-853, 1976.
- [15] Pitas I., *Digital Image Processing Algorithms*, Prentice Hall, New York, 1993.
- [16] Grytskiv Z., Voloshynovskiy S., Rytsar Yu., "A median regularization of iterative image restoration methods", *Proc. SPIE in Optoelectronic and Hybrid Optical/Digital Systems for Image Processing*, vol. 3238, pp. 29-37, 1997.
- [17] Yung N.H.C., Lai A.H.C., Poon K.M., "Modified CPI Filter Algorithm for Removing Salt-and-Pepper Noise in Digital Images", *Proc. SPIE in Visual Communication and Image Processing'96*, vol. 2727, pp. 1439-1449, 1996.